Time-Lapse Tomography of A Longwall Panel: A Comparison of Location Schemes

Kray Luxbacher, Graduate Research Assistant
Erik Westman, Associate Professor
Virginia Tech
Blacksburg, VA

Peter Swanson, Geophysicist
NIOSH-Spokane Research Laboratory
Spokane, WA

ABSTRACT

Three-dimensional time-lapse velocity tomograms were generated to image stress redistribution around a longwall panel to produce a better understanding of the mechanisms that lead to ground failure. Mining-induced microseismic events provided passive sources for the three-dimensional velocity tomography. Surface-mounted geophones monitored microseismic activity for 18 days.

Most similar studies have utilized active sources including longwall shearers, controlled explosions, and hammer blows. These active sources generally require a person to initiate and measure the location and time of the source, and are not conducive to continuous monitoring. This method utilizes mining induced microseismic events as passive sources and lends itself well to continuous monitoring.

Two event location methods were compared in order to move toward quantification of tomographic results in terms of ground conditions. Additionally, LAMODEL was utilized to determine the expected stress distribution around the longwall panel and compare these images to the velocity tomograms. Eighteen tomograms were generated, one per day, and high velocity regions in the set of tomograms generated from the initial location algorithm correlated with abutment stress redistribution predicted by numerical modeling.

This research is significant as it has the potential to improve safety in underground mines and is the only example of long term passive velocity tomography implementation for the purpose of inferring stress redistribution around an area of active mining. Though still immature, this technology has the potential to allow mine personnel to image areas of active mining on a regular basis and detect areas with anomalous velocity distributions indicating potential safety hazards.

INTRODUCTION

As the mining industry develops ore deposits in increasingly challenging conditions, ground control remains one of the most important aspects of mine planning and operation. Three of four fatalities that occurred in underground coal and metal/nonmetal mines between January I, 2007 and May I, 2007 were the result of roof falls (I). Unplanned roof falls pose a considerable risk to miners and can hinder production substantially. Currently, real time assessment of roof conditions generally includes visual observation, some localized measurements of movement, and, in some cases, monitoring of microseismic events (2).

Seismic tomography allows for inference of stress distribution through a velocity image. Seismic velocity tomography is a noninvasive technology that can be used to determine rock mass response to ore removal. Velocity tomography is accomplished by propagating seismic waves through a rock mass to measure velocity distribution of the rock mass. Specifically, the P-wave arrival time is measured. Tomograms are created by mapping this velocity distribution in three dimensions. The three-dimensional velocity model can then be sliced in areas of interest, such as the active working level, resulting in a two-dimensional tomogram, and relative stress in the rock mass can be inferred.

Velocity tomography is an appropriate technology for the study of rockbursts, events that occur in underground mines as a result of excessive strain energy being stored in a rock mass, and sometimes culminating in violent failure of the rock. Rockbursts often involve inundation of broken rock into open areas of the mine, which can result in injury, blocked travelways, and unplanned ventilation changes.

This research has the potential to improve safety in underground mines by allowing mine personnel to image areas of active mining on a regular basis and detect areas where velocity distributions seem unusually high or atypical in location.

BACKGROUND

Previous Work

While seismic tomography has been applied frequently in oil and gas exploration and in earthquake studies the application is far less prevalent in the mining industry.

When seismic tomography is applied to mining, active sources are generally used. Active sources have also been implemented repeatedly to image individual pillars in underground mines (3-8). Tunnels have also been imaged to determine stress distribution

around an excavation implementing both passive (9, 10) and active sources (1 1).

The aforementioned studies are conducted on a relatively small scale where active sources and optimum source-receiver placement are fairly easy to implement. There are fewer large scale mine studies in the literature. Friedel and others used active sources to span drifts and image high velocity in working faces (12). Rootbolt-mounted receivers have been implemented with a longwall shearer as a source to image a section of a longwall panel (13). An earlier study was able to image velocity on a longwall panel and show that high velocity areas advanced with the longwall face (14).

In combination with an array that surrounds the volume of interest, active sources allow for optimal seismic ray coverage. Ray coverage is an important parameter in seismic tomography. Poor spatial coverage will result in smeared features. Additionally, ray density impacts the resolution or sharpness of the image. Denser ray coverage provides more data for the velocity model, so that each voxel or pixel in the image is better constrained. A large seismic wavelength, relative to voxel size, can also have an adverse effect on resolution (15).

Source Location

Active source tomography is not a realistic option for long-term mine monitoring because it is generally labor intensive. The method presented here utilizes mining-induced microseismic events as passive sources, lending itself well to continuous monitoring. However, disadvantages of passive sources are the inability to constrain the spatial distribution of sources, and event locations depend upon the unknown velocity structure that is sought in the model. These disadvantages result in error in source location. This error is difficult to quantify and can significantly influence the velocity distribution in the tomogram. It is imperative that various location schemes be examined to determine their effects on velocity tomograms.

Case Study

The rock mass under investigation in this research is the strata surrounding an underground coal mine in the western United States, utilizing longwall mining. Eighteen days of microseismic data were collected by NIOSH in 1997. Instrumentation consisted of sixteen receivers mounted on the surface approximately 365 meters above the longwall panel of interest. The system recorded and located the microseismic events.

The active coal seam is 2.6 to 3.0 meters thick and is underlain and overlain by massive sandstone units. The longwall panel was 250 meters wide and retreated about 431 meters over the course of the 18-day study.

Original Event Location Method

Initially, event locations were calculated using an iterative solution technique with a spatial-gradient basis function (16). A minimum of ten P-wave arrival times were used in each solution. An initial isotropic layered velocity model was constructed using nearby available sonic logs as a starting point. Average velocity values and the positions of five model layer boundaries were chosen to best approximate the sonic logs. Calculations using this initial model located a majority of the events below the seam and not in the known layers of sandstone caving directly above the seam. With a surface array that is essentially flat, and the use of only P-wave arrival times, there is little constraint on the vertical position of calculated event locations approximately 365 meters below the surface. Therefore, velocity values were subsequently adjusted to constrain the median depth of the activity to just above the mining horizon. Constraints for these adjustments were provided by array-based velocity calibration measurements in near-identical geologic strata above the same seam in other parts of the mine several kilometers away. The resulting model is shown in Figure 1.

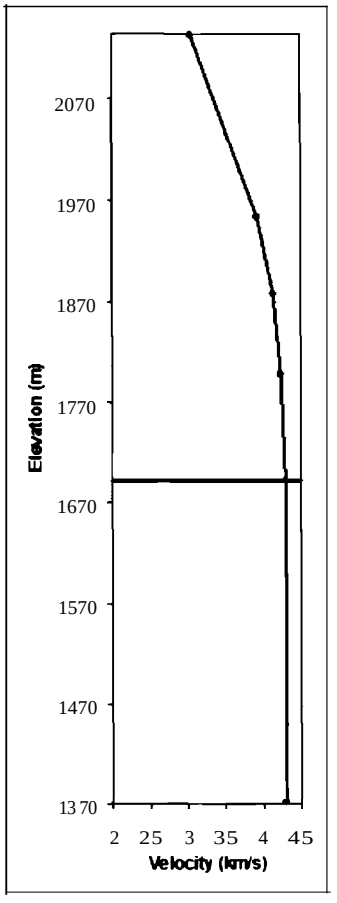

Figure 1. Initial isotropic layered velocity model.

Double-Difference Event Locations

Double-difference location (17) refers to the difference between calculated and observed seismic travel times for a pair of microseismic events. If two microseismic events have very similar travel times at all stations then they are defined as a pair, because it is assumed that they will also have very similar raypaths. Next, the distance between the two events, which, presumably, is much smaller than the distance from the event to the receiver, is iteratively adjusted to reach a solution which accounts for the difference in travel times for the pair while minimizing the difference between the calculated and observed travel times.

There are several examples of double difference relocation in the literature (18-19). However, all of these examples are related to volcanic and earthquake activity with no specific application to mining.

Inversion

The inversion procedure used to generate the velocity tomograms, can only occur once the passive sources, microseismic events, have been located. Velocity tomography is based on the relationship between time, distance, and velocity of a ray traveling through a medium. The mass is discretized and the velocity is determined for each discrete unit of the mass, a voxel, in the three-dimensional case.

The principal equation is (20):

$$T=DP \rightarrow P=D^{-1}T \qquad (1)$$

Where T is a matrix of travel times per ray, D is a matrix of distances per ray per voxel, and P is a matrix of slowness (inverse velocity) in each grid cell. Inversion of the matrix D should allow for a relatively simple solution.

Most tomography problems are ill-posed – they have no unique solution. This usually results in a singular distance matrix, for which there is no inverse, so iterative solutions are often employed. Consideration of *a priori* information allows for the better solutions to be chosen. This information often includes an initial velocity model determined through exploration of the rock mass. This initial model can then be iteratively perturbed until a solution is found that fits the data.

A commercial package was utilized for the inversion of the data. The data were inverted using both the initial microseismic event locations and the double-difference microseismic event locations. GeoTOM implements the Simultaneous Iterative Reconstruction Technique, SIRT, to accomplish the inversion (21). SIRT (22) can require a large number of iterations, but is generally more stable than some of the other iterative techniques.

The Velocity-Stress Relationship

In laboratory testing of rocks P-wave velocity increases slightly with initial axial stress. Prior to the peak stress the elastic wave velocity begins to decrease rapidly as microcracks propagate (23), so that an increase in velocity would be indicative of an increase in stress, but a decrease in velocity is not necessarily indicative of failure - it may be a pre-failure indicator. Thill indicates changes in P-wave velocity are largely due to changes in cracks and porosity (24). Other factors also affect the P-wave velocity, including fluid saturation which can increase the wave speed (25) and preferred orientation of cracks which can give rise to velocity anisotropy. It is vital that the velocity-stress relationship is carefully considered when using velocity tomograms to make inferences about relative stress in a mine.

EXPERIMENTAL PROCEDURE

The original data set provided microseismic event locations, receiver locations and measured arrival times for each source-receiver pair. For each event, the first arrival time was set to zero, so that the subsequent arrivals were timed relative to the first arrival. Travel times through the layered velocity model were then calculated for each event-receiver pair. These travel times were calculated using TTBOX (26), an algorithm that computes seismic ray paths and travel times for a one-dimensional spherical velocity model.

For double difference microseismic event locations, the calculated travel time data is read into HypoDD (27), a double difference event location program developed by Waldhauser, and the events are relocated. The original event locations and subsequent HypoDD locations are displayed in Figure 2 relative to the longwall panel geometry.

The HypoDD event locations and calculated travel times were inverted using a commercial package that utilizes SIRT and produces a three-dimensional velocity model. A smoothing constant of 0.02 was applied in all directions and 12 curved ray iterations were performed for each day. Travel time residuals were deemed to be suffiently stable after 12 iterations. The smoothing constant constrains the velocity in each voxel in relation to the neighboring voxels in order to avoid high or low velocity artifacts in areas with poor seismic ray coverage.

Finally, the three-dimensional model was input into a commercial three-dimensional visualization program. In this phase, any voxels bisected by less than five rays were removed from display. The program interpolates between well constrained voxels to determine velocity over the entire model. This also minimizes high velocity artifacts in the model which can be misleading.

The initial set of tomograms, using the first location method. were processed in the same way with two exceptions. First, the travel times were calculated for straight ray paths, so they are probably less realistic than the TTBOX travel times because they do not take into account raybending due to velocity change. Also. the initial event locations were used for this set.

RESULTS AND DISCUSSION

Event Locations

The initial event locations are shown in gray with the double difference locations in black in relation to the pillar geometry and longwall face locations in Figure 2. Events are scaled by relative magnitude. Mining is retreating from the northeast to the southwest. The tailgate is the northern gateroad, while the headgate is the southern gateroad. The panel adjacent to the tailgate was previously mined.

The initial event locations are consistently in front of the mining face with a few events in the gob and along the tailgate. In days 2, 5, and 7 the double difference microseismic event locations are fairly similar to the initial locations, although they may be more tightly clustered. However, the double difference microseismic event locations differ significantly from the initial locations on days 12, IS, and 18. The microseismic events located by the double difference algorithm migrate east into the gob, and on day 12 they also migrate south over the headgate. The double difference microseismic event relocations seem improbable in comparison with the initial locations. A previous study of microseismic events at a longwall mine in the western United States determined that most microseismic events occurred in the forward stress abutment zone (28). Although there is significant activity in the gob as the roof collapses behind the longwall shields these failures are often in tension, and produce far less energy than the compressional failures occurring in front of the face. The samestudy suggested that these high energy compressional failures were more likely to be picked up by the microseismic system (28).

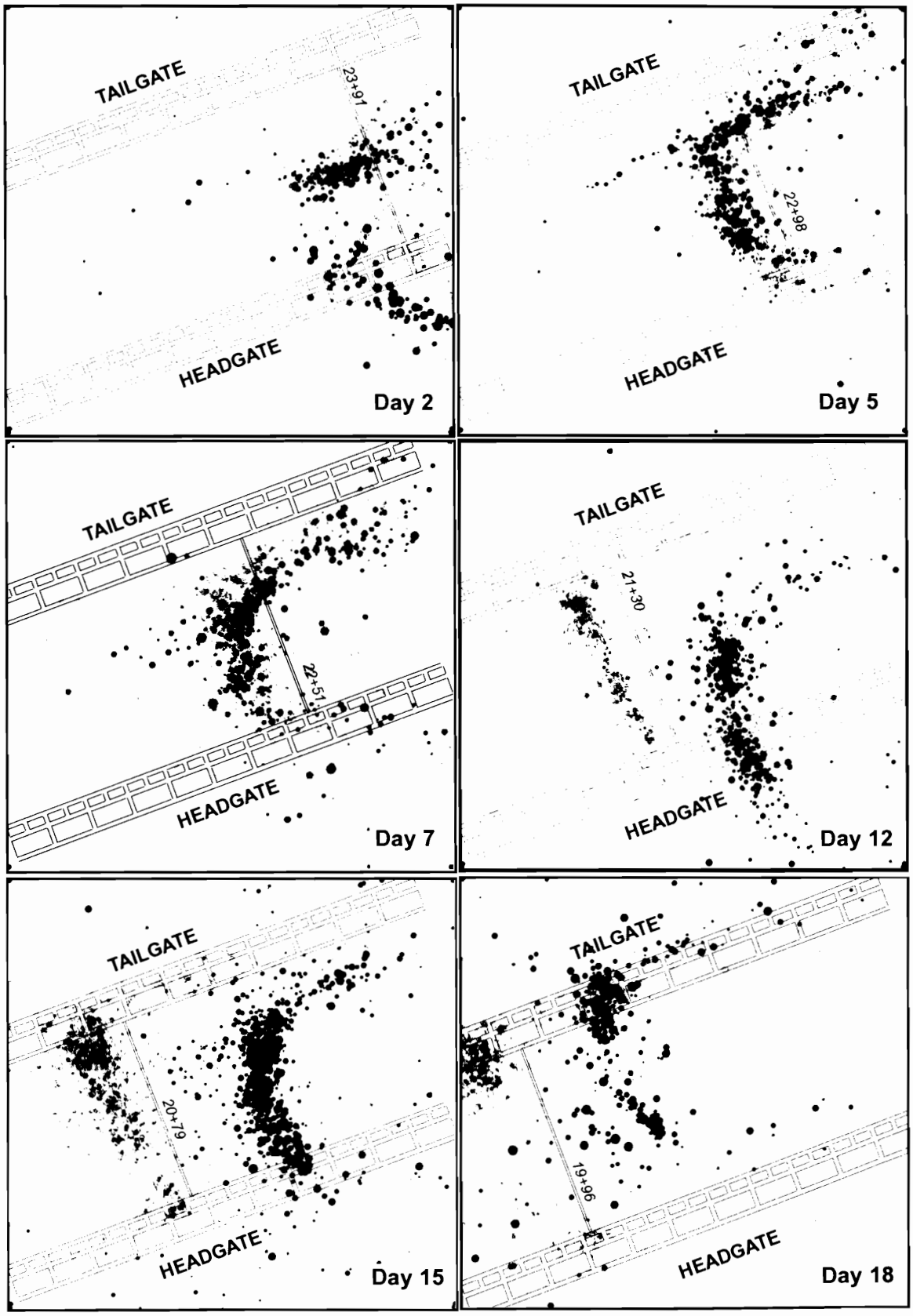

Figure 2. Plan view of microseismic event locations in relation to the longwall geometry. The initial microseismic event locations are displayed in gray, while the double difference microseismic event locations are displayed in black. The events are plotted by relative magnitude. Stations are displayed in meters for the face locations.

Figure 2 does not display the vertical change between the two location schemes, but the double difference microseismic location algorithm shifted the events toward the surface in all six cases. This may account for the lateral shift of events, because the distance had to be increased to satisfy the theoretical arrival time. Since all of the receivers were surface-mounted this vertical location is poorly constrained.

Seismic Velocity Tomograms

The velocity tomograms generated from the initial locations and from the double difference locations are displayed in Figures 3 and 4, respectively. These tomograms are plan views, sliced at approximately seam level, with the longwall excavation geometry overlain. In Figure 3, tomograms generated from the initial microseismic event locations, a high velocity zone, represented by darker colors, is distinguishable just in front of the longwall face and along the tailgate, and is observed to advance with the face.

The tomograms generated from the events that were located with the double difference algorithm display a large area of low velocity at the face and tailgate, with a high velocity area visible well in front of the face on days 2 and 5, near the left edge of the tomograms. These tomograms seem unlikely to represent the true state of the rock mass for several reasons. First, days 2 and 5 are the only days that seem to exhibit any redistribution of high velocity features with face retreat. Additionally, the presence of these features on days 2 and 5 is uncertain because there is very poor ray coverage in that area of the model, so those voxels are not well constrained. Also, because the double difference algorithm forced the event locations toward the surface the voxels at seam level in Figure 4 are less well-constrained than the same voxels in Figure 3. Finally, the double difference microseismic event location scheme eliminates events that are relocated above the surface and events that are not paired with other events (27). The ray coverage for the tomograms in Figure 3 is denser than for the tomograms in Figure 4. The number of events used for each set of tomograms is displayed below in Table I.

Table 1. Occurrence of events and number of events remaining after the final relocation iteration.

Day	No. of Events used in initial location	No. of Events used in HypoDD location
2	430	395
5	591	514
7	739	589
12	819	671
15	1450	1157
18	666	578

Also, it is evident in Table1 that ray coverage is substantially denser on some days due to the number of microseismic events that were recorded.

There are some substantial limitations in both methods. First, the initial isotropic, layered, model is a gross simplification of actual ground conditions and does not reflect the low-velocity region association with caving and gob areas that advance through the rock mass in a time-dependent fashion. Next, calculation of event locations and travel times based on this simplified model results in systematic errors and eventually leads to distortion in the velocity images.

Numerical Modeling

Two LAMODEL plots, from days 5 and 12, are displayed in Figure 5 to compare the expected stress pattern with the observed velocity patterns. The highest stresses are displayed in light colors in the forward abutment zone and in the gateroad pillars, especially on the tailgate. The LAMODEL plots show the expected forward abutment stress, and some tailgate abutment stress. These plots appear to correlate more closely with the initial location velocity tomograms.

CONCLUSIONS

The initial location scheme seems to correlate most closely with the LAMODEL plots, and also illustrates velocity redistribution with face retreat. The tomograms displayed in Figure 3 are probably a more realistic estimate of the state of the rock mass than the tomograms displayed in Figure 4. The presence of high velocities in the abutment zones, and their subsequent redistribution indicates that this technology is promising as a tool for inferring the stress state in a mine.

Additionally, the comparison of the initial microseismic event location scheme and the double difference microseismic event location scheme indicates that event locations significantly affect velocity tomograms. Although the double difference location scheme did not generate reasonable event locations this is probably a function of the oversimplified initial velocity model than evidence of an inappropriate algorithm. Further study of these schemes to determine the most appropriate algorithm or algorithms for locating microseismic events is vital for creating a viable real-time velocity imaging system in a mine.

These tomograms do not exhibit the smooth and continuous redistribution of stress that might be expected. There are several reasons for this; first, the distribution and number of microseismic events significantly affect the images. Since passive sources are employed this is not a parameter that can be controlled. Some images are generated from more data with better coverage than others. Also, a representative sample of the 18 days of data are shown here to illustrate the velocity change over the course of the study, so tomograms are not displayed for consecutive days. It is significant that with the original location scheme high velocity features were imaged that can be observed to redistribute with longwall face retreat.

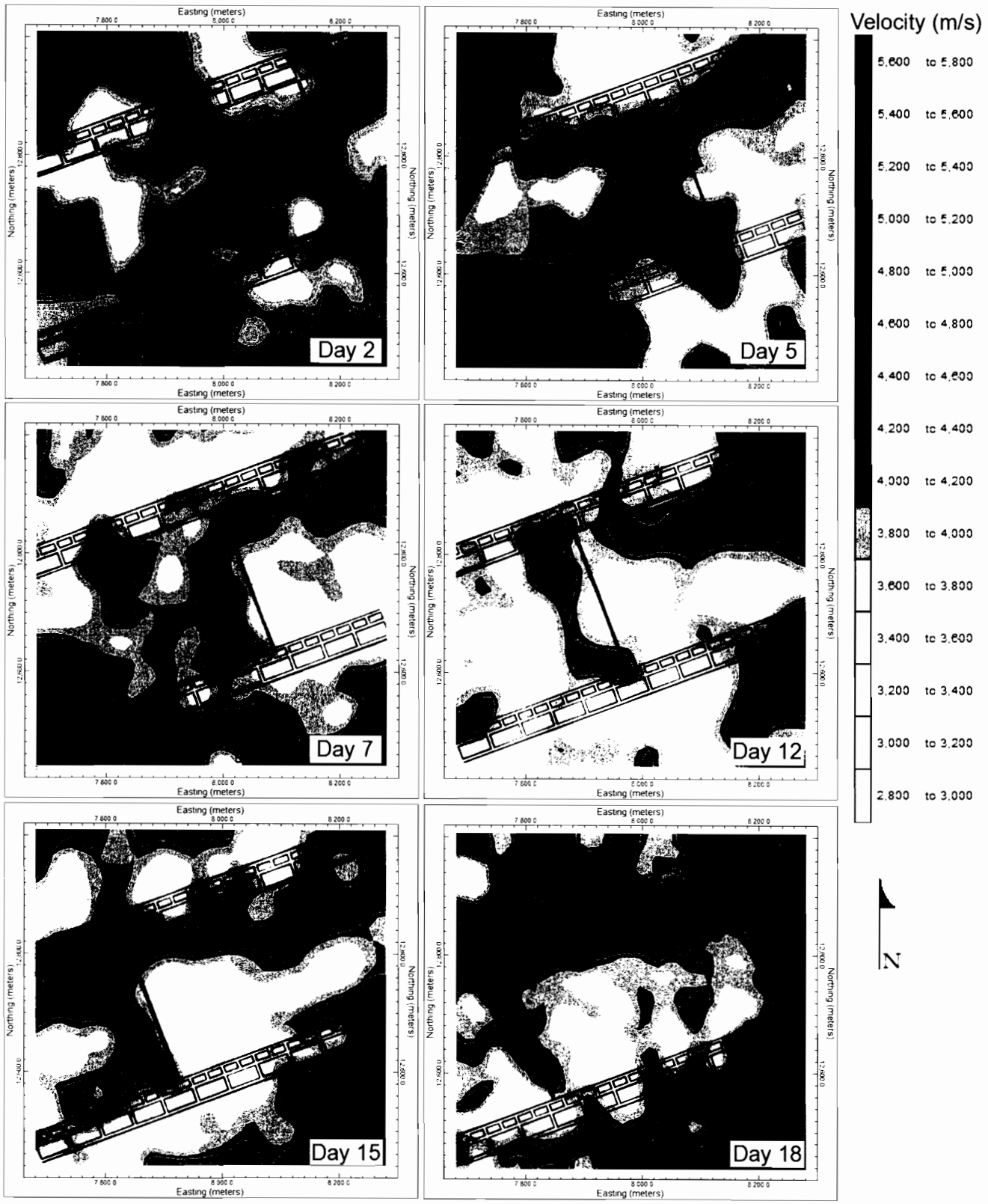

Figure 3. Plan view velocity tomograms at seam level. Days 2, 5, 7, 12, 15, and 18 are shown. The longwall face is retreating in the southwest direction. The initial event location algorithm was used prior to inverting this data.

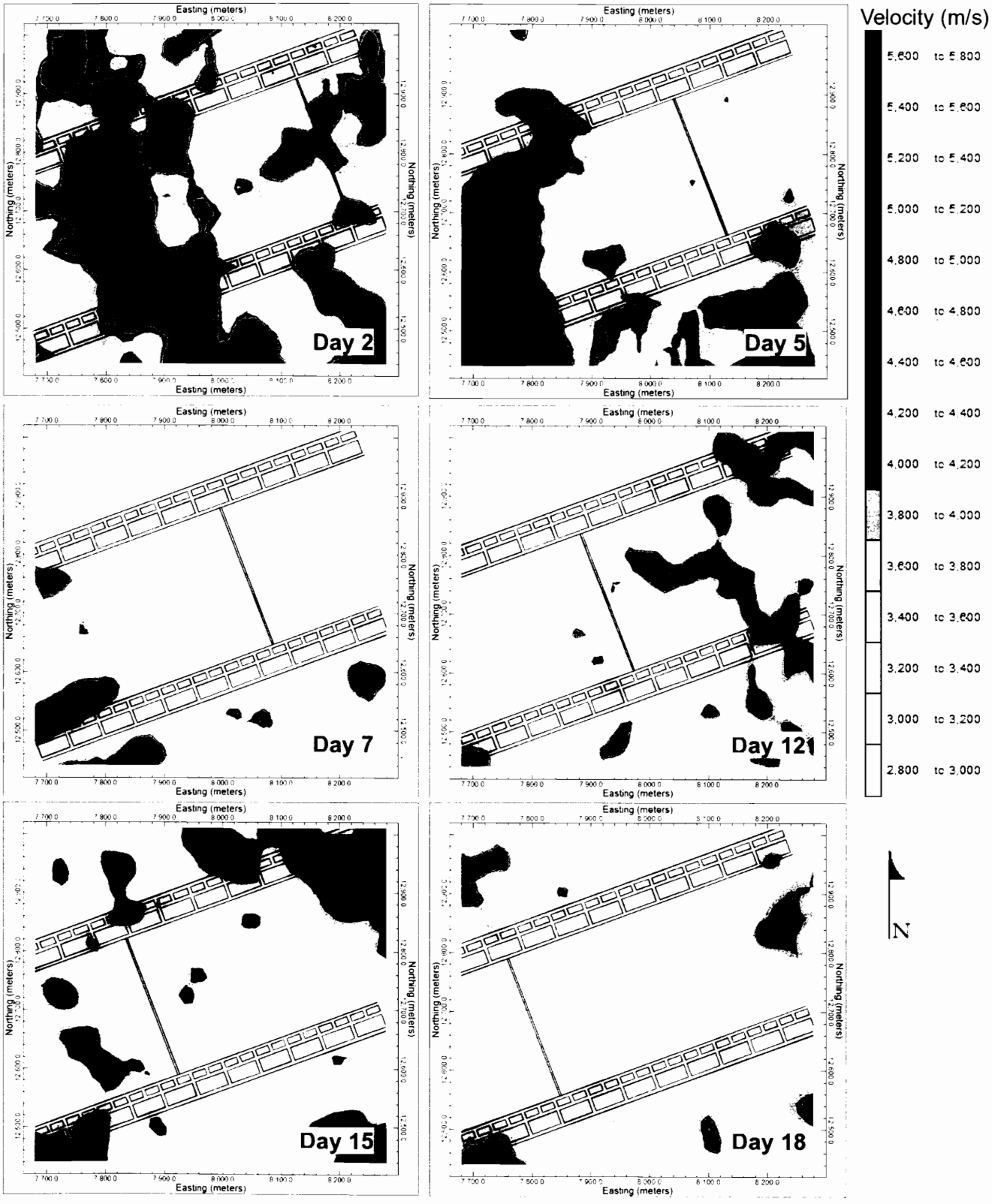

Figure 4. Plan view velocity tomograms at seam level. Days 2, 5, 7, 12, 15, and 18 are shown. The longwall face is retreating in the southwest direction. The double difference event location algorithm was used prior to inverting this data.

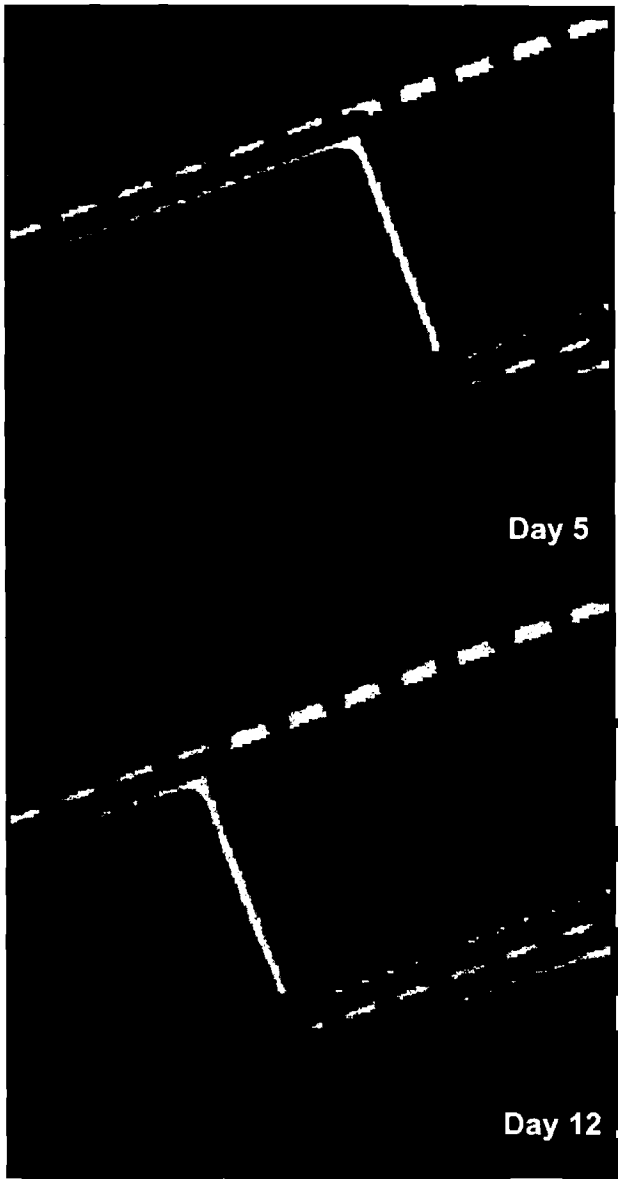

Figure 5. Plan view LAMODEL stress plots of the longwall panel at seam level for days 5 and 12 of the study. The highest stresses are represented by the light color in the forward abutment zone, and in the gateroad pillars.

Future Research

Future research will involve use of TomoDD (29), a program that combines the HypoDD location algorithm with an inversion, optimizing both the location and the inversion. TomoDD simultaneously inverts for the event locations and the velocity structure, which mitigates some of the error that occurs as a result of using an oversimplified initial velocity model to calculate travel times.

Synthetic tomography of the LAMODEL plots could also yield information about the validity of the velocity tomograms exhibited here. A synthetic velocity tomogram of the theoretical stress distribution displayed in a LAMODEL plot would provide information about how stress features might be misrepresented or smeared due to inadequate ray coverage. In order to generate synthetic tomograms a theoretical velocity-stress relationship must be established, and then travel times will be calculated based on the actual event locations. Finally, the same inversion process will be used to detennine how closely the velocity tomogram models the LAMODEL stress plot.

Successful velocity imaging of stress distribution in underground mines could lead to routine imaging of velocity distribution in mine roof, providing miners and mine operators with additional infonnation about the stress state of the mine and enhancing safety and production.

ACKNOWLEDGEMENTS

The authors are grateful to NIOSH for providing the data for this study. This research is funded by a National Science Foundation CAREER Grant (CMS-0134034).

REFERENCES

(I) MSHA, Fatalities Year-to-Date: Coal & MetallNonmetal. 2007. Mine Safety & Health Administration. www.msha.gov: Accessed May 3, 2007.

(2) Iannacchione, A., T. Bajpayee, and J. Edwards. Forecasting Roof Falls with Monitoring Technologies. Proceedings, 24th International Conference on Ground Control in Mining, West Virginia University, Morgantown, WV, Aug. 2-4, 2005, pp. 44-51.

(3) Maxwell, S.C., and R.P. Young. "A Comparison between Controlled Source and Passive Source Velocity Images." Bulletin of the Seismological Society of America 83, no. 6 (1993): 1813-1834.

(4) Friedel, M.J., M.J. Jackson, E.M. Williams, M.S. Olson, and E. Westman. Imaging of Coal Pillar Conditions: Observations and Implications." *International Journal of Rock Mechanics, Mining Science, and Geomechanics Ahstracts* 33, no. 3 (1996): 279-290.

(5) Manthei, G. "Seismic Tomography on a Pillar in a Potash Mine." Paper presented at the Proceedings of the 4th International Symposium on Rockbursts and Seismicity in Mines, Krakow, Poland, August 11-14 1997.

(6) Scott, D. F., 1.M. Girard, T. J. Williams, and D. K. Denton. "Comparison of Seismic Tomography, Strain Relief, and Ultrasonic Velocity Measurements to Evaluate Stress in an Underground Pillar." In *Mining, Metallurgy, and Exploration. Inc. Annual Meeting.* Denver, Colorado: SME, 1999.

(7) Scott, D.F., T.J. Williams, D. Tesarik, D.K. Denton, S.J. Knoll, and 1. Jordan. "Geophysical Methods to Detect Stress in Underground Mines: Report of Investigations." NIOSH, Spokane Research Laboratory, 2004.

(8) Watanabe, T., and K. Sassa. "Seismic Attenuation Tomography and its Application to Rock Mass Evaluation." *International Journal of Rock Mechanics, and Mining Sciences* 33, no. 5 (1996): 467-477.

(9) Maxwell, S.C., and R.P. Young. "A Controlled Insitu Investigation of the Relationship between Stress, Velocity and Induced Seismicity." *Geophysical Research Leiters* 22, no. 9 (1995): 1049-1052.

(10) Maxwell, S.C., and R.P. Young. "Seismic Imaging of Rock Mass Responses to Excavation." *International Journal of Rock Mechanics, Mining Sciences, and Geomechanics Abstracts* 33, no. 7 (1996): 713-724.

(11) Meglis, l.L., T. chow, C.D. Martin, and R.P. Young. "Assessing in Situ Microcrack Damage Using Ultrasonic Velocity Tomography." *International Journal of Rock Mechanics, Mining Science, and Geomechanics.* 42 (2004): 25-34.

(12) Friedel, MJ., D.F. Scott and TJ. Williams. "'Temporal Imaging of Mine-Induced Stress Change Using Seismic Tomography." Engineering Geology 46, no. 2 (1997): 131-141.

(13) Westman, E.C., K.Y. Haramy, and A.D. Rock. "Seismic Tomography for Longwall Stress Analysis." Paper presented at the *Proceedings of the 15th International Conference on Ground Control in Mining,* Golden, Colorado. 1996.

(14) Kormendi, A., T. Bodoky, L. Hermann, L. Dianiska, and T. Kalman. Measurements for Safety in Mines." *Geophysical Prospecting* 34, no. 7 (1986): 1022-1037.

(15) Williamson, P.R. and M. H. Worthington. limits in ray tomography due to wave behavior: Numerical experiments." Geophysics 58, no. 5 (1993): pp. 727-735.

(16) Estey, L., P. L. Swanson, F. M. Boler, and S. Billington. Microseismic Event Locations: A Test of Faith. Paper in Proceedings of the 31 st U. S. Symposium on Rock Mechanics. Colo. Sch. of Mines, Golden, CO, 1990, pp. 939-946.

(17) Waldhauser, F. and W.L. Ellsworth. "A Double-Difference Earthquake Location Algorithm: Method and Application to the Northern Hayward Fault, California." *Bulletin of the Seismological Society of America,* 90, no. 6, pp. 1356-1368.

(18) Veilleux, A.M. and 0.1. Doser. "Studies of Wadati-Benioff zone seismicity of the Anchorage, Alaska region." *Bulletin of the Seismological Society of America,* 97, no. 1B (2007), pp. 52-62.

(19) Meyer, N., H. Deshon, C. Thurber, and S. Prejean. "Cross-correlation and double-difference techniques used in earthquake relocations at Shishaldin Volcano, Alaska." Seismological Research Letters, 77, no. 2 (2006), pp. 241.

(20) Jackson, MJ., and D.R. Tweeton. - Geophysical Tomography Using Wavefront Migration and Fuzzy Constraints; Report of Investigations 9497." United States Bureau of Mines, 1994.

(21) Tweeton, D. and Running the Three-Dimensional Tomography Program Geotomcg." Apple Valley, MN: Geo Tom, LLC, 200 I.

(22) Dines, K.A. and RJ. Lytle. Geophysical Tomography." *Proceedings of the IEEE* 67, n07 (1979): 1065-1074.

(23) Paterson, M.S. and Wong, T-F. Experimental rock deformation, the brittle field. Berlin: Springer, 1978.

(24) Thill, R.E. Methods for Monitoring Failure in Rock." Paper presented at eh 14th Symposium on Rock Mechanics, University Park, PA 1973.

(25) Toksoz, M.N., C.H. Cheng, and A. Timur. "Velocity of Seismic Waves in Porous Rocks." Geophysics 41, no 4 (1976): 621-645.

(26) Knapmeyer, M. "Numerical Accuracy of Travel-time Software in Comparison with Analytic Results." Seismological Research Letters, 76, no 1 (2005), pp. 74-81.

(27) Waldhauser, F. "hypoDD - A Program to Compute Double Difference Hypocenter Locations." Open File Report, U.S. Geological Survey (200 I).

(28) Heasley, K.A., J.L. Ellenberger, and P.W. Jeran. An Analysis of Rock Failure Around a Deep Longwall Using Microseismics. Proceedings, 20th International Conference on Ground Control in Mining, West Virginia University, Morgantown, WV, Aug. 7-9,2001, pp. 280-286.

(29) Zhang, H. and C. Thurber. manual for tomoDD 1.1 (double-difference tomography) for determining event locations and velocity structure form local earthquakes and explosions." Dept. of Geology and Geophysics, University of Wisconsin, Madison, (2003).